Pediatric Oncology

9

M. Eiber, L. Merlini, O. Ratib, K. Scheidhauer,
M. Souvatzoglou, C. Tabouret-Viaud, and T. Zand

Contents

M. Eiber (✉)
Department of Radiology, Klinikum Rechts der Isar,
Technische Universität München, Munich, Germany
e-mail: matthias.eiber@tum.de

L. Merlini
Division of Pediatric Radiology, Department of Medical Imaging,
Geneva University Hospitals, Geneva, Switzerland

O. Ratib
Division of Nuclear Medicine and Molecular Imaging,
Department of Medical Imaging, Geneva University Hospitals,
Geneva, Switzerland

K. Scheidhauer • M. Souvatzoglou
Department of Nuclear Medicine, Technische Universität München,
Munich, Germany

C. Tabouret-Viaud
Division of Nuclear Medicine and Molecular Imaging,
Department of Medical Imaging, Geneva University and Geneva
University Hospitals, Geneva, Switzerland

T. Zand
Division of Pediatric Radiology, Department of Medical Imaging,
Geneva University and Geneva University Hospitals,
Geneva, Switzerland

Pediatric Oncology

In pediatric oncology ^{18}F-FDG PET/CT imaging is used mainly for staging and restaging of lymphoma and soft tissue and bone tumors. In this special patient collective minimizing the radiation dose is one of the major goals. With the introduction of PET/MR, the CT exposure component previously produced in PET/CT studies potentially can be eliminated [1]. Preliminary reports state that compared to PET/CT the radiation exposure from a single hybrid imaging PET/MR-scan is reduced by around 80 %, to only one effective dose of 4.6 mSv [2, 3]. In addition, especially in bone tumors (e.g. Ewing-sarcoma, multifocal osteosarcoma) patient require both whole-body MR and ^{18}F-FDG PET and, therefore, the combination of both examinations in one single session has also substantial logistical advantages (e.g. only one anesthesia).

Furthermore, compared to PET/CT this technique also enables whole-body diffusion-weighted imaging (DWI) providing additional information about cellularity and nuclear/cytoplasmic ratio of tumors. Recent studies in pediatric patients with lymphoma demonstrated high sensitivity for the detection of lesions and allows quantitative assessment of diffusion that may aid in the evaluation of malignant lymphomas [4]. For soft-tissue and bone tumors the advantage of PET/MR compared to PET/CT also lies in its high soft-tissue contrast [5]. ^{18}F-FDG PET/CT does not provide exact information as MRI for T-staging in sarcomas, however it can give additional prognostic information [6, 7]. e.g. in one study assessing therapy response in pediatric osteosarcomas ^{18}F-FDG PET could discriminate responders from nonresponders [8]. In regards of the advantages of both modalities integrated PET/MRI can replace PET/CT for these indications with a focus of the ^{18}F-FDG PET component for prognostic questions and assessment of N-stage and M-stage and the MR-examination on local staging.

O. Ratib et al. (eds.), *Atlas of PET/MR Imaging in Oncology*,
DOI 10.1007/978-3-642-31292-2_9, © Springer-Verlag Berlin Heidelberg 2013

Follow-up of Intestinal Adenocarcinoma

Clinical History

Seventeen-year-old patient after surgery and chemotherapy of a mucinous intestinal adenocarcinoma with complete remission 21 months after seven cycles of chemotherapy. Follow up study for staging of possible recurrence of an abdominal mass.

Imaging Technique

PET: Whole-body PET acquired 60 min after injection of 369 MBq of ^{18}F-FDG, 57 kg/157 cm patient, with 5.2 mmol/L of fasting glycemia.

MRI: Whole body atMR (T1 weighted), supine position. 3D Dixon, T2 weighted and STIR whole-body MRI.

Findings

PET/MR images confirmed the recurrence of tumoral tissue in a polymorphic mass in the pre-sacral area with combined solid and cystic components and increased FDG uptake in the sold parts of the tumor.

Teaching Points

While MR may sometimes be limited for evaluation of abdominal masses, PET/MR may provide adequate evaluation of solid masses in follow up of young patients avoiding unnecessary radiation from multiple PET/CT studies.

Fig. 9.1 Coronal MIP reconstruction of PET images shows multiple focal areas of FDG uptake in the abdomen and mild diffuse uptake in the colostomy located on the right

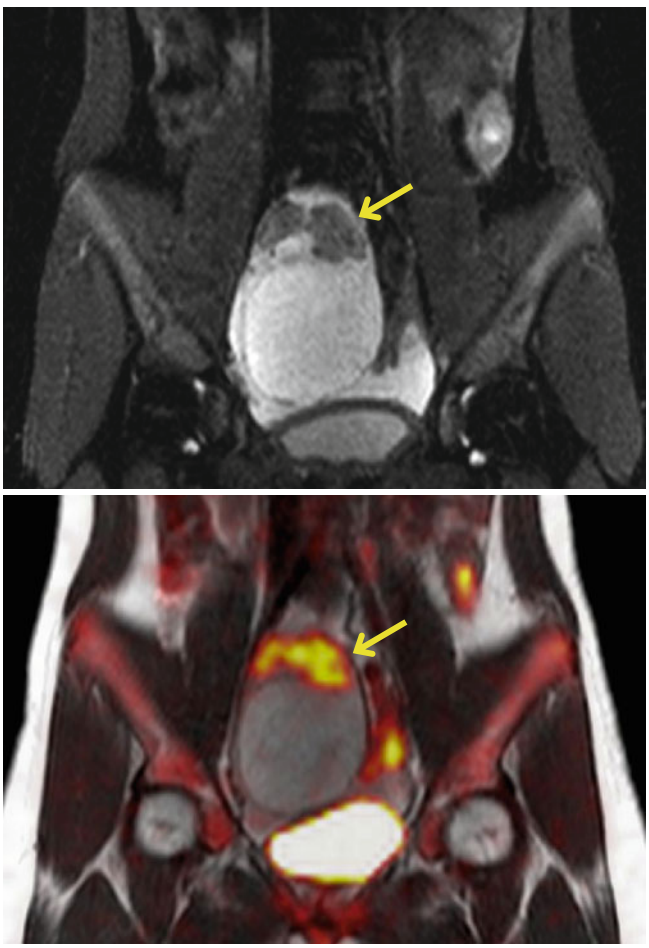

Fig. 9.2 Coronal STIR MR (*top*) and T2 weighted TSE PET/MR (*bottom*) images of the retro-peritoneal mass (*arrow*) with cystic and solid components with increased focal uptake of FDG

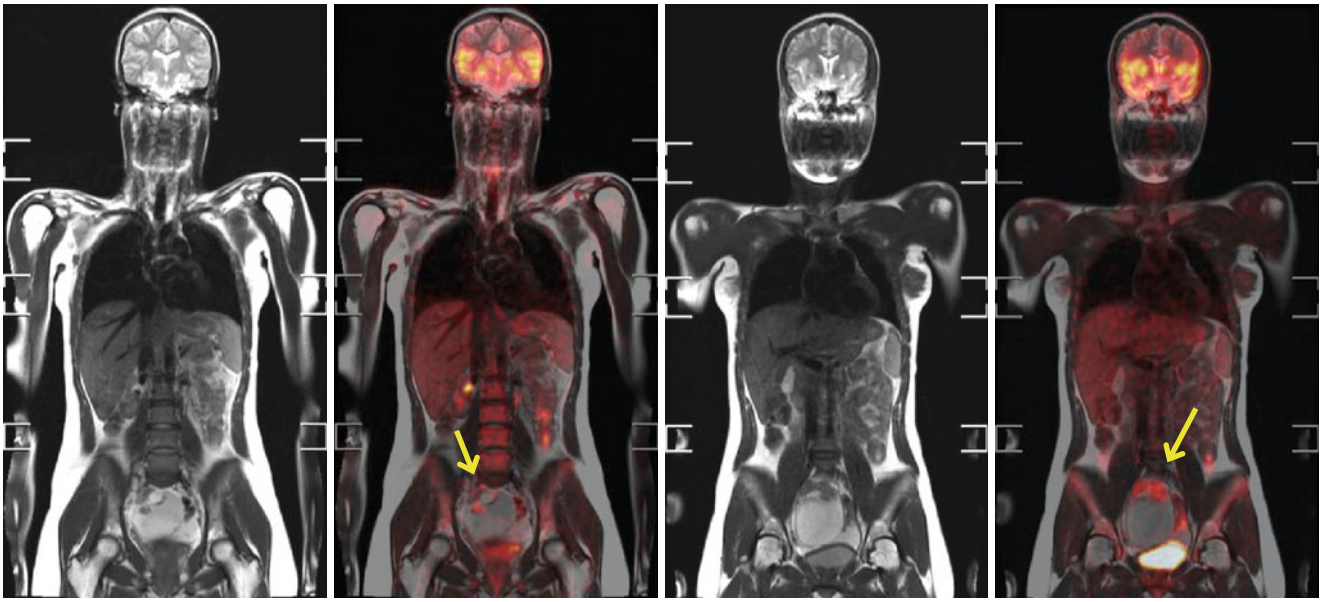

Fig. 9.3 Whole-body coronal T2 weighted TSE MR images fused with corresponding PET images showing the localization of the retro-peritoneal mass (*arrow*)

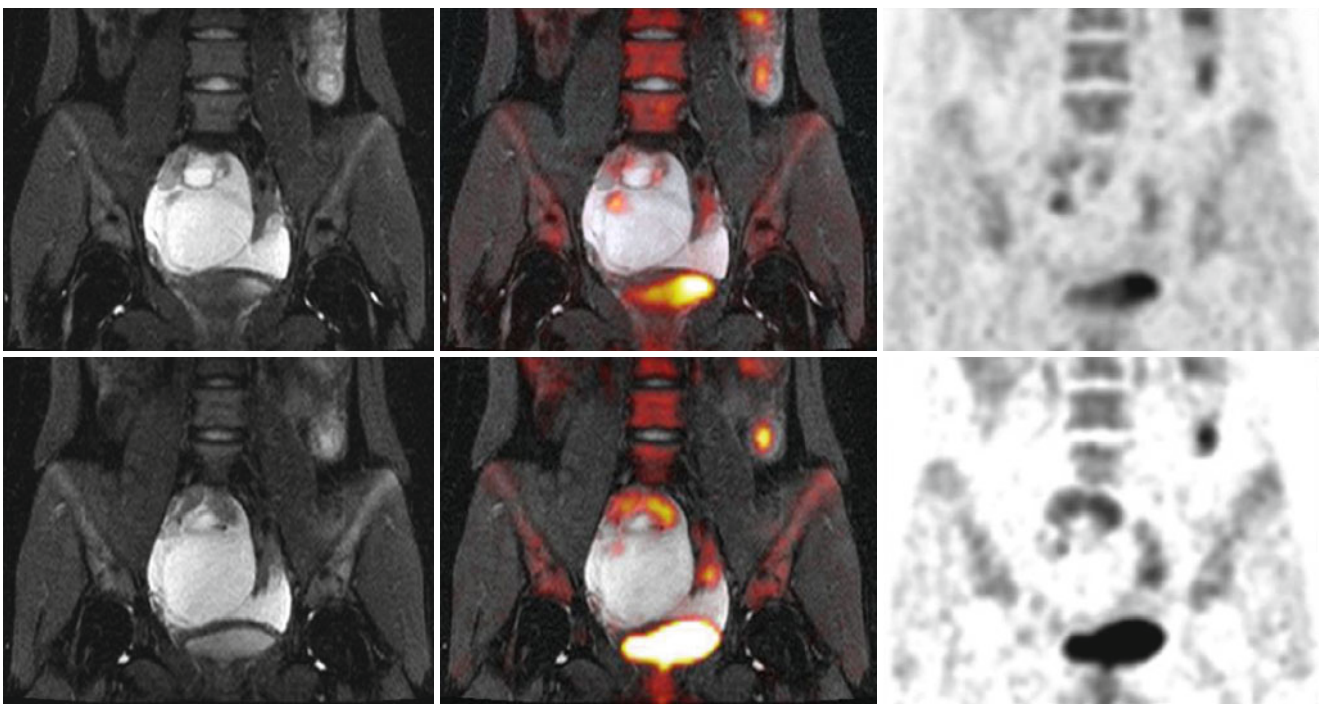

Fig. 9.4 Two adjacent coronal planes of STIR MR sequences fused with PET images of the same location showing the heterogeneous composition of the pelvic mass with a large cystic component

Follow-up of Renal Cyst

Clinical History

Sixteen-year-old patient followed for a left renal cyst since 2001 with a recent change in morphology that could suggest malignant transformation.

Imaging Technique

PET: Whole-body PET acquired 60 min after injection of 370 MBq of ^{18}F-FDG.

MRI: Whole body atMR (T1 weighted), supine position. 3D Dixon and T2 weighted whole-body MRI . Followed by diagnostic MRI, with HASTE diffusion and eThrive sequences.

Findings

PET/MR showed a normal study without evidence of abnormal tracer uptake at the level of the cyst or in any other distant lymph nodes.

Teaching Points

PET/MR could replace PET/CT in pediatric cases where exclusion of malignant tumors is required with the added value of combining of PET's negative predictive value and the ability of MRI for tissue and lesion characterization.

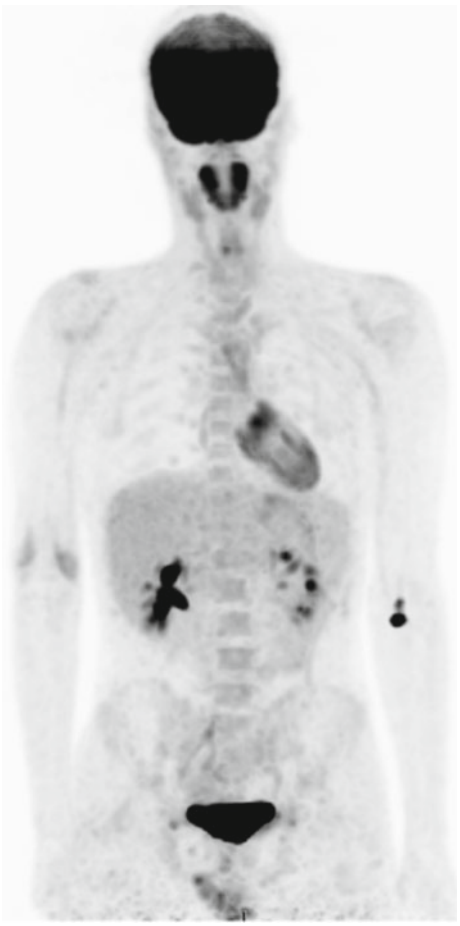

Fig. 9.5 Coronal MIP reconstruction of PET images with no evidence of abnormal PET uptake in the kidney or abdomen

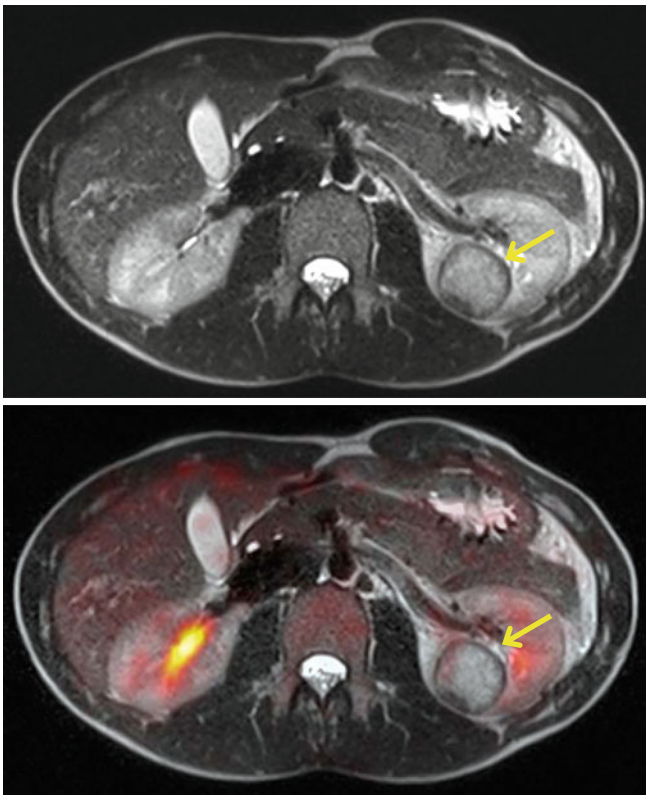

Fig. 9.6 Axial respiratory gated T2 weighted HASTE (*top*) and fusion with corresponding PET image (*bottom*) with no abnormal tracer uptake around the renal cyst (*arrow*)

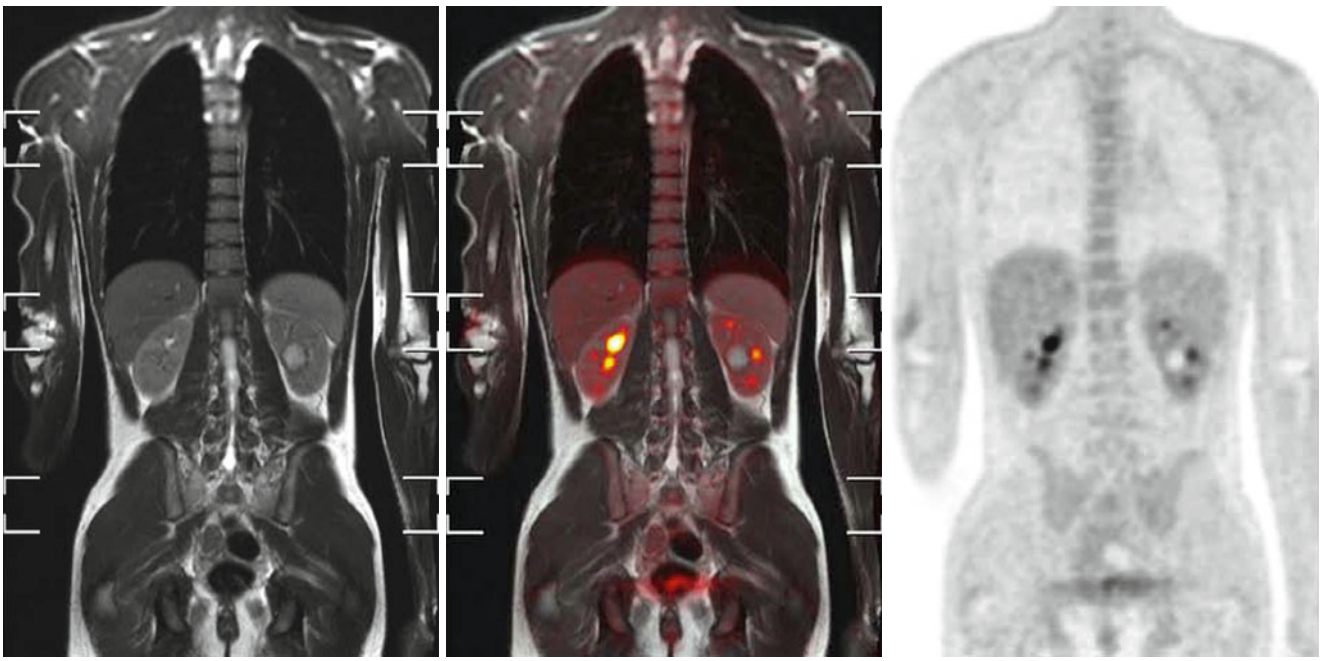

Fig. 9.7 Coronal reformatted images from whole-body T2 weighted TSE images fused with corresponding PET images showing no abnormal tracer uptake

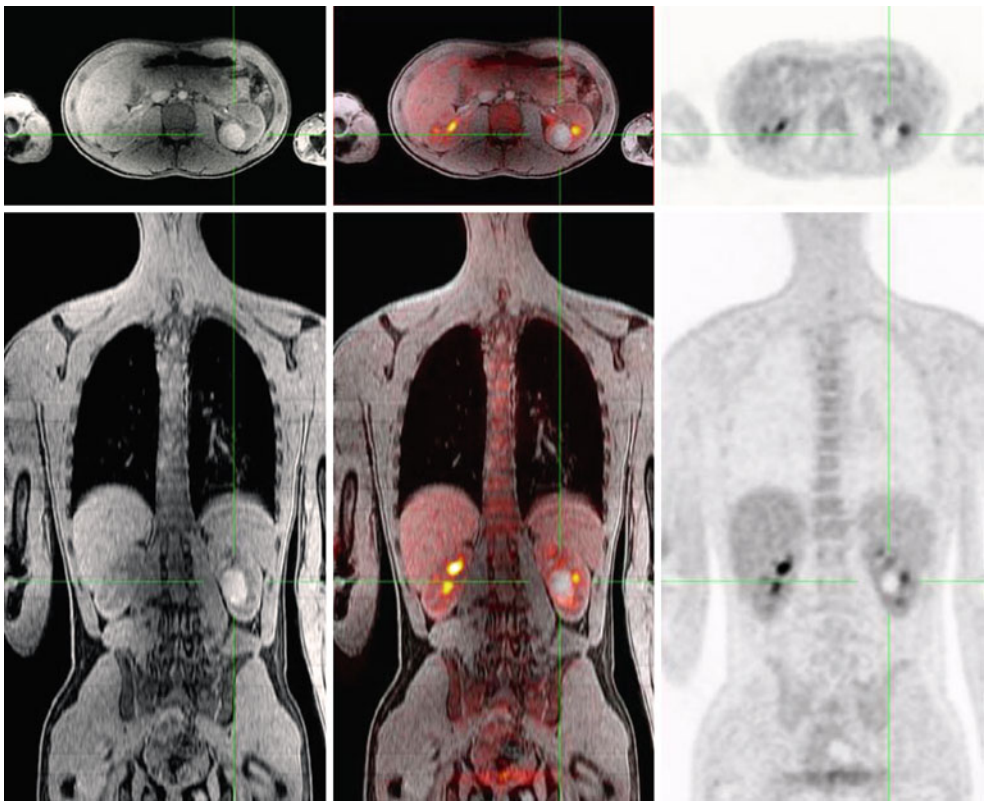

Fig. 9.8 Multiplanar reformatting of whole-body 3D Dixon sequence at the level of the renal cyst

Follow-up Post Treatment of Hodgkin Disease

Clinical History

Sixteen-year-old patient after treatment by chemotherapy for Hodgkin disease. Assessment of end of treatment.

Imaging Technique

PET: Whole-body PET acquired 60 min after injection of 370 MBq of ^{18}F-FDG.

MRI: Whole body atMR (T1 weighted), supine position. 3D Dixon, DWIBS and T2 weighted whole-body MRI sequences.

Findings

PET/MR showed a normal study with complete regression of mediastinal mass seen on the PET/CT study performed prior to initiating chemotherapy treatment.

Teaching Points

PET/MR could replace PET/CT in pediatric follow up studies for assessment of the efficacy of oncological treatments.

PET/MR fusion allows better differentiation of lymph node tracer uptake and brown fat uptake of FDG.

Fig. 9.9 Coronal MIP reconstruction of PET images with no evidence of abnormal tracer uptake. Note the diffuse heterogeneous uptake in brown fat (*arrows*)

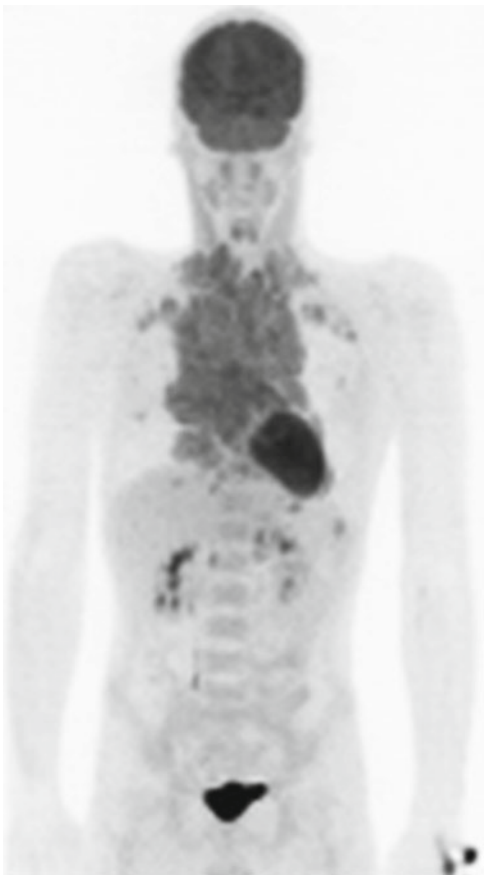

Fig. 9.10 Comparative whole body PET study prior to chemotherapy showing the large mediastinal mass of Hodgkin lymphoma

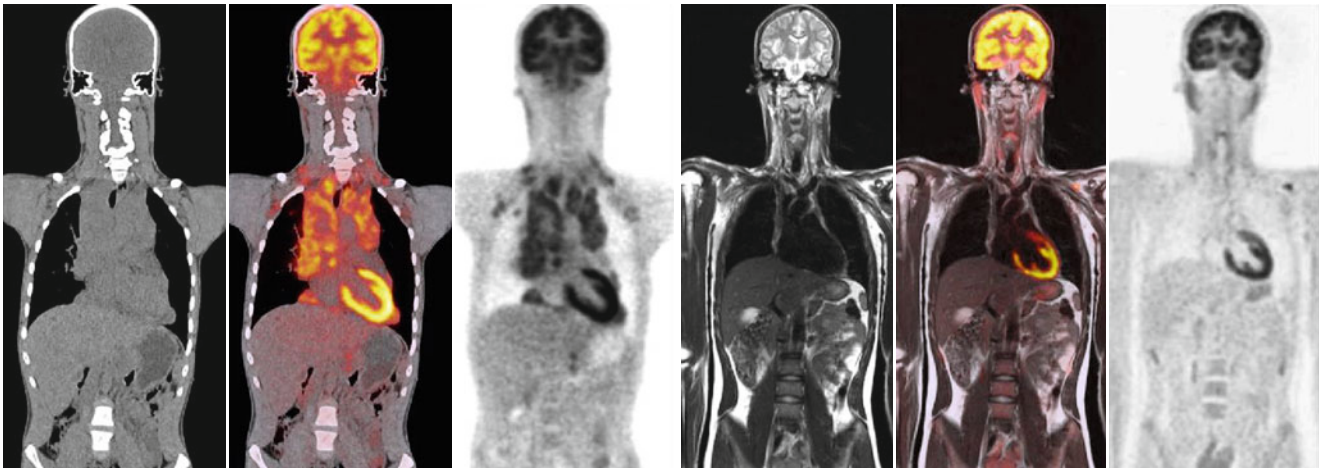

Fig. 9.11 Comparison of pre-treatment PET/CT study (*left*) and post chemotherapy PET/MR study (*right*) showing complete response to therapy with disappearance of all mediastinal masses

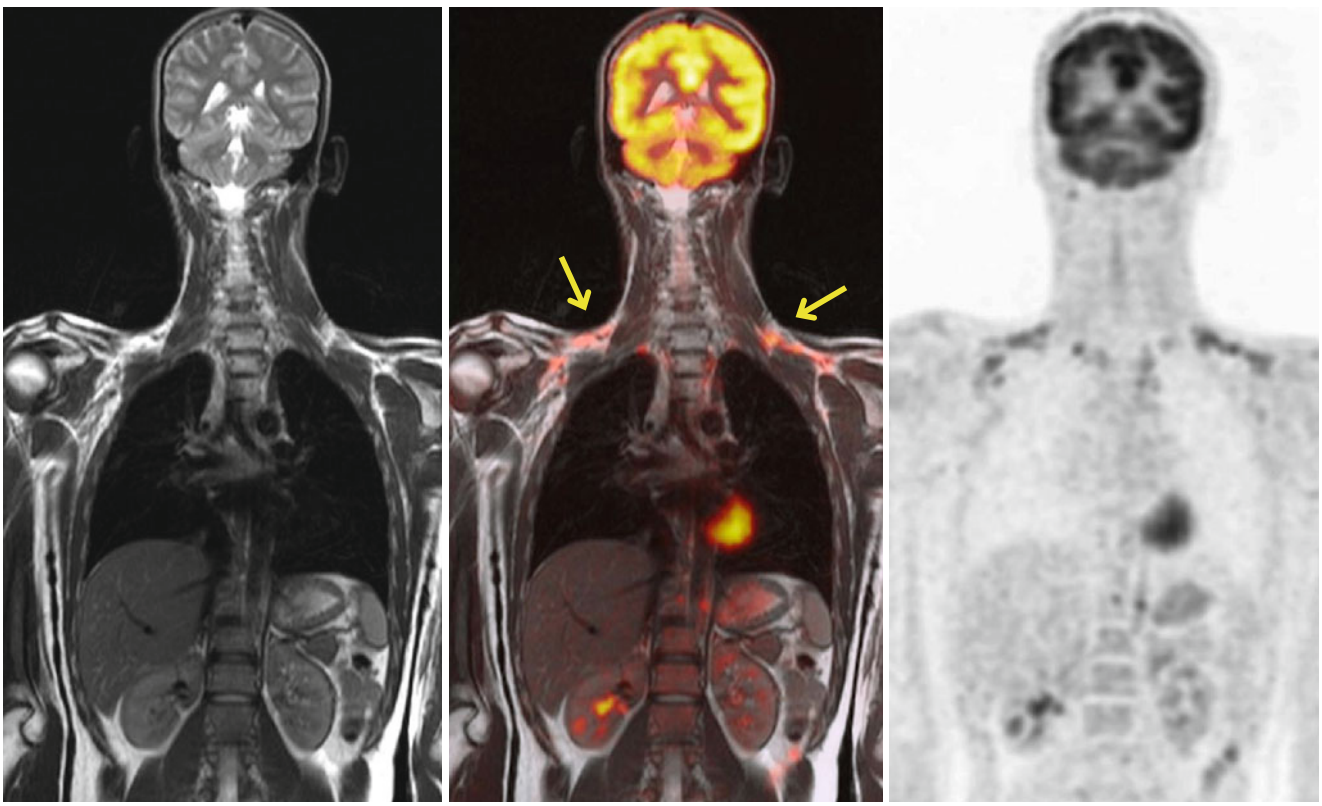

Fig. 9.12 Coronal fused images of PET/MR showing the localization of brown fat uptake (*arrows*)

Long-Term Follow-up of Hodgkin Disease

Clinical History

Fifteen-year-old patient referred for follow-up 2 years after treatment by chemotherapy and radiotherapy for Hodgkin disease.

Imaging Technique

The acquisition was performed on a Philips whole-body hybrid Ingenuity TF PET/MR scanner.

PET: Whole-body PET acquired 60 min after injection of 370 MBq of ^{18}F-FDG.

MRI: Whole body atMR (T1 weighted), supine position. 3D Dixon, STIR and T2 weighted whole-body MRI sequences.

Findings

PET/MR showed a normal study with complete regression of thoracic enlarged lymph nodes seen on the PET/CT study performed prior to initiating treatment.

Teaching Points

PET MR could replace PET/CT in pediatric follow up studies for assessment of the efficacy of oncological treatments particularly in lymphoma patients.

PET/MR fusion allows better differentiation of lymph node tracer uptake and brown fat uptake of FDG.

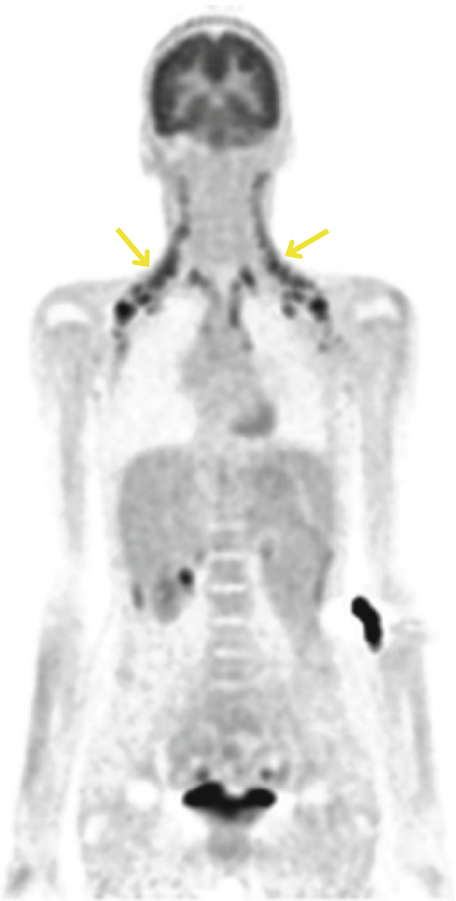

Fig. 9.13 Coronal MIP of PET images with no evidence of abnormal tracer uptake, except physiological uptake in brown fat (*arrows*)

Fig. 9.14 Comparative whole body PET study performed 2 years earlier prior to treatment showing multiple hypermetabolic lymph nodes of Hodgkin lymphoma

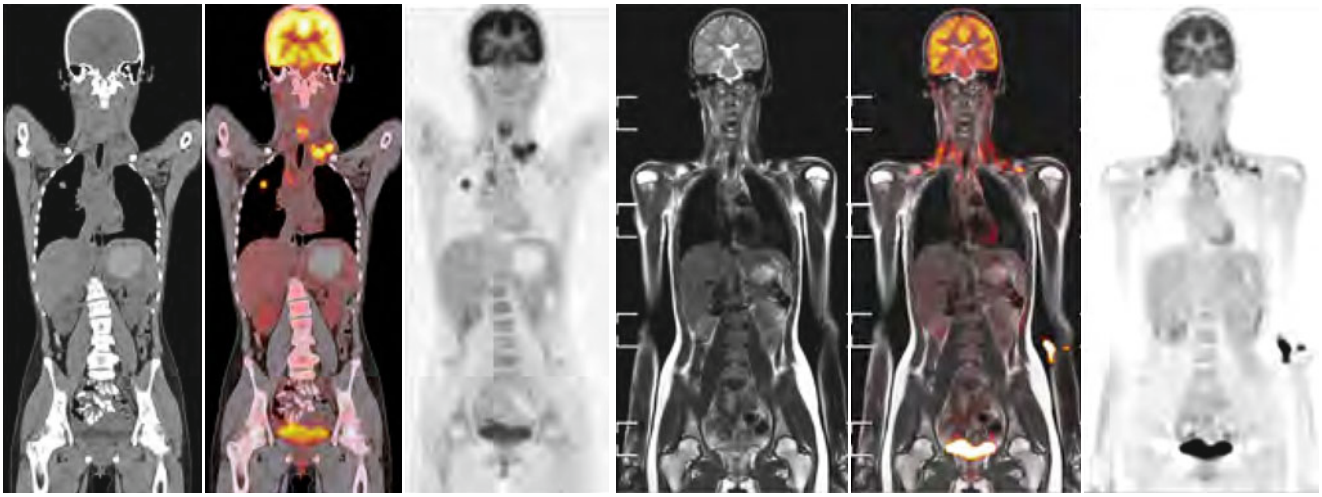

Fig. 9.15 Comparison of pre-treatment PET/CT study (*left*) and 2 years follow-up post treatment PET/MR study (*right*) showing complete response to therapy. Focal FDG uptake bilaterally correspond to physiological brown fat uptake

Fig. 9.16 Coronal fused images of PET/MR showing the localization of brown fat uptake (*arrows*)

Fig. 9.17 Coronal fused whole-body images showing no abnormal focal uptake except brown fat uptake

PET/MR in Langerhans Cell Histiocytosis

Clinical History

A 12-year-old patient presents with pain in the left hip since several weeks. A prior X-ray revealed an osteolytic lesion in the left ileal bone suspicious for Langerhans cell histiocytosis.

Imaging Technique

Whole body PET/MR images acquired 135 min after iv injection 335 MBq 18F-FDG, 58 kg.

8 beds × 3 min together with whole body cor T2w STIR. 1 bed (pelvis) a 15 min together with cor T1w TSE before and after Gadolinium, ax T2w TSE and ax T1w fs TSE after Gadolinium. Additional sequences for the brain: ax T2w flair and MPRage after Gadolinium. Head/neck and four body coils.

Findings

Besides extensive activity due to brown fat a PET/positive lesion with intense contrast enhancement is demonstrated in the left ileal bone. No other suspicious lesions could be visualized both in MRI and PET.

Teaching Points

The combination of whole-body PET and MR can aid in excluding or confirming the presence of multiple lesions in Langerhans cell histiocytosis. This is essential information for the clinician in the further treatment of those patients.

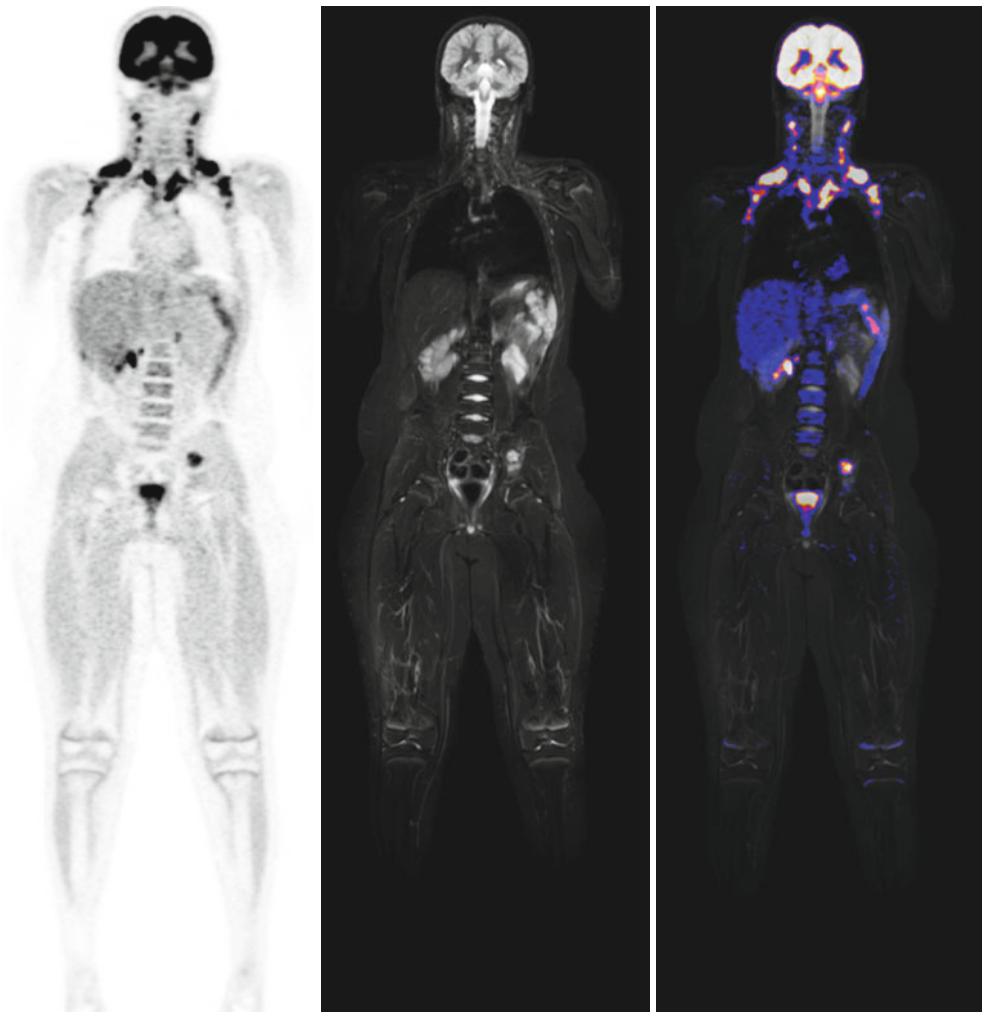

Fig. 9.18 Coronal whole body PET demonstrates intense FDG-accumulation due to brown fat. In addition a focal moderate uptake could be found in the left ileal bone (*left*). In the whole body coronal T2w STIR sequence only one lesion is confirmed by a hyperintense signal (*middle*). Additional fusion between coronal T2w stir and PET shows a good correlation between the single lesion in PET and MRI (*right*)

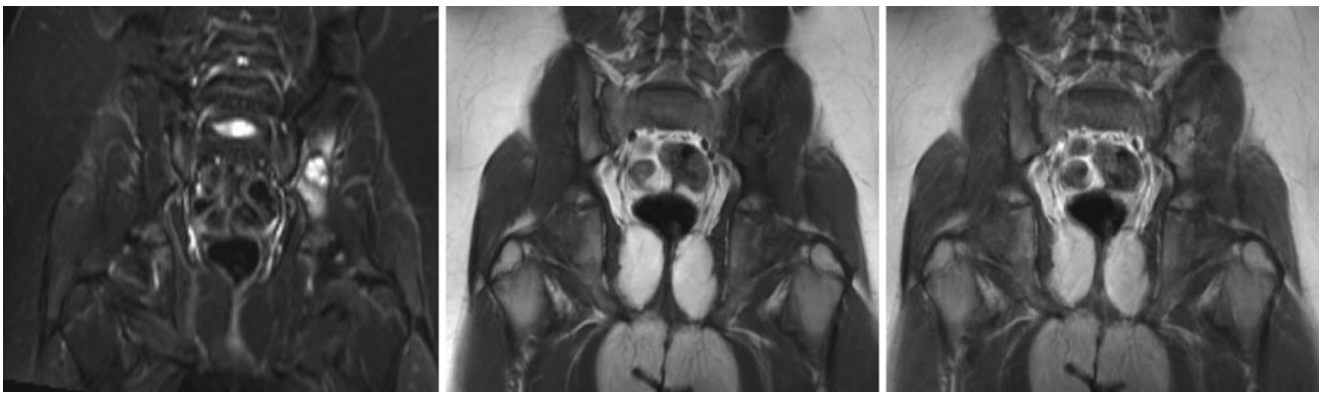

Fig. 9.19 Coronal T2w STIR reveals a hyperintense lesion in the right ileal bone with surrounding edema (*left*). Corresponding coronal T1w TSE demonstrate moderate to intense contrast enhancement of the lesion (*middle* and *right*)

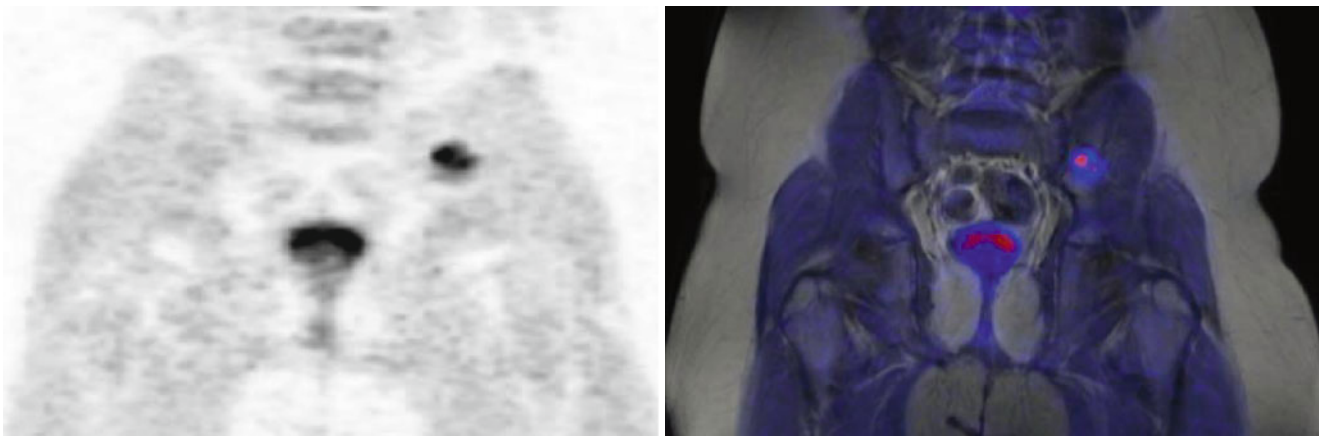

Fig. 9.20 Coronal PET (*left*) and fused images (*right*) show a good anatomical correlation between the moderate increased focal FDG-metabolism and the abnormality in MRI

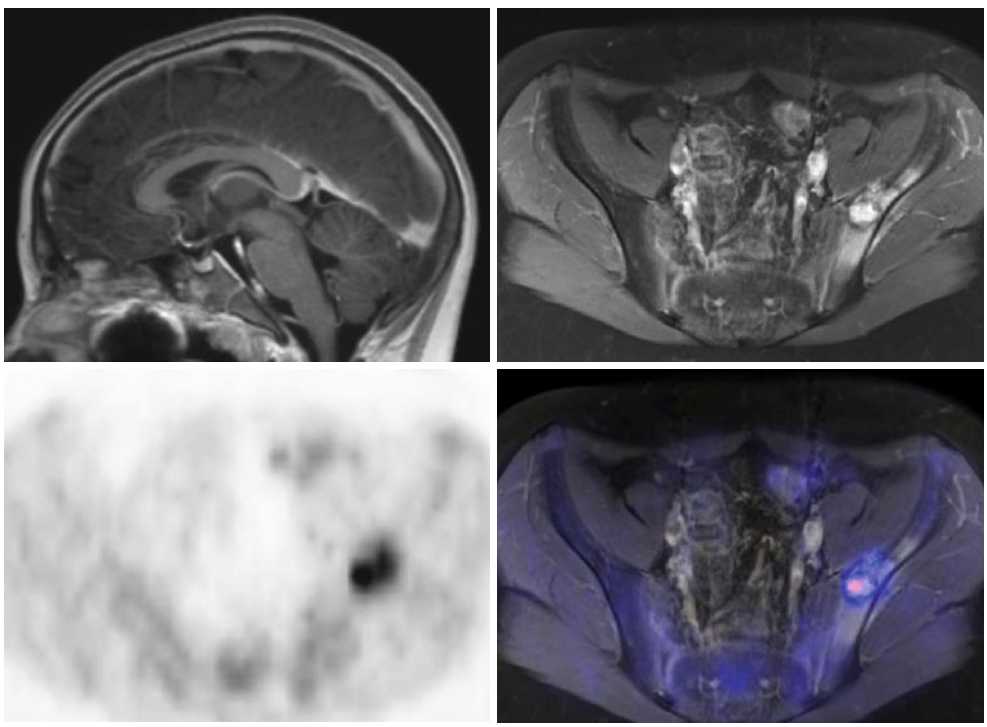

Fig. 9.21 No involvement of the brain espc. the hypophyseal stalk can be found in the sagittal reformatted MPR age after Gadolinium (*top left*). The anatomical extent of the lesion in the left ileal bone is outlined in the axial T1w TSE fs after Gadolinium sequences (*top right*). Axial PET and fused images demonstrate the highest uptake in PET in the region of the most intense contrast enhancement (*lower row*)

Ewing Sarcoma

Clinical History

Eleven year old boy with a large symptomatic tumor of the left pelvis, a histologically proven Ewing sarcoma of the left os ilium.

Imaging Technique

Whole body PET/MR images acquired pre- and post-therapy 135 min (Fig. 9.22), resp. 140 min (Fig. 9.23) after i.v injection of 198 MBq, resp. 123 MBq 18F-FDG, 27 kg.

7 beds × 3 min together with coronal T2 STIR and coronal T1 TSE. T1 VIBE Dixon for attenuation correction.

Findings

High FDG-uptake of the primary Ewing sarcoma of the left os ilium, corresponding to the T1-hypointense tumor lesion shown in Fig. 9.22.

Images acquired 8 month later after RCTx show no more tracer uptake in the lesion. MRT shows residual tumor lesion in the left os ilium exhibiting hypointense signal in the T1-sequence.

Teaching Points

FDG-PET is able to demonstrate good therapeutic response of the treatment indicating no active tumor. MRT shows the large decrease of the lesion size. Combination of PET and MR could be a valuable tool assessing the response to therapy of bone tumors. Images also show the conversion to fatty bone marrow in the lumbar spine after RCTX, in contrast to the thoracic spine.

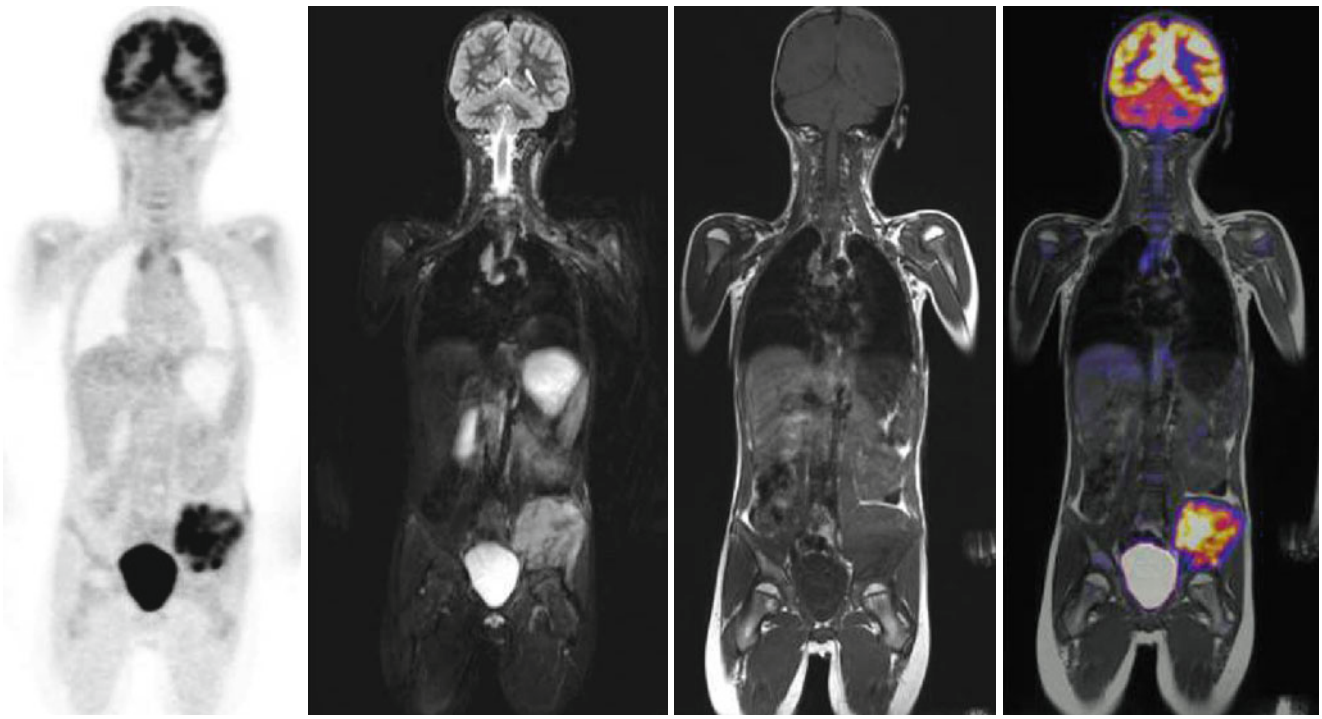

Fig. 9.22 Coronal T1 TSE whole body shows a hypointense homogenous lesion of the left os ilium, infiltrating the soft tissue structures of the pelvis. The space occupying lesion is hyperintense in the T2 STIR. PET shows an intensive glucose utilization of the whole tumor, no other lesions

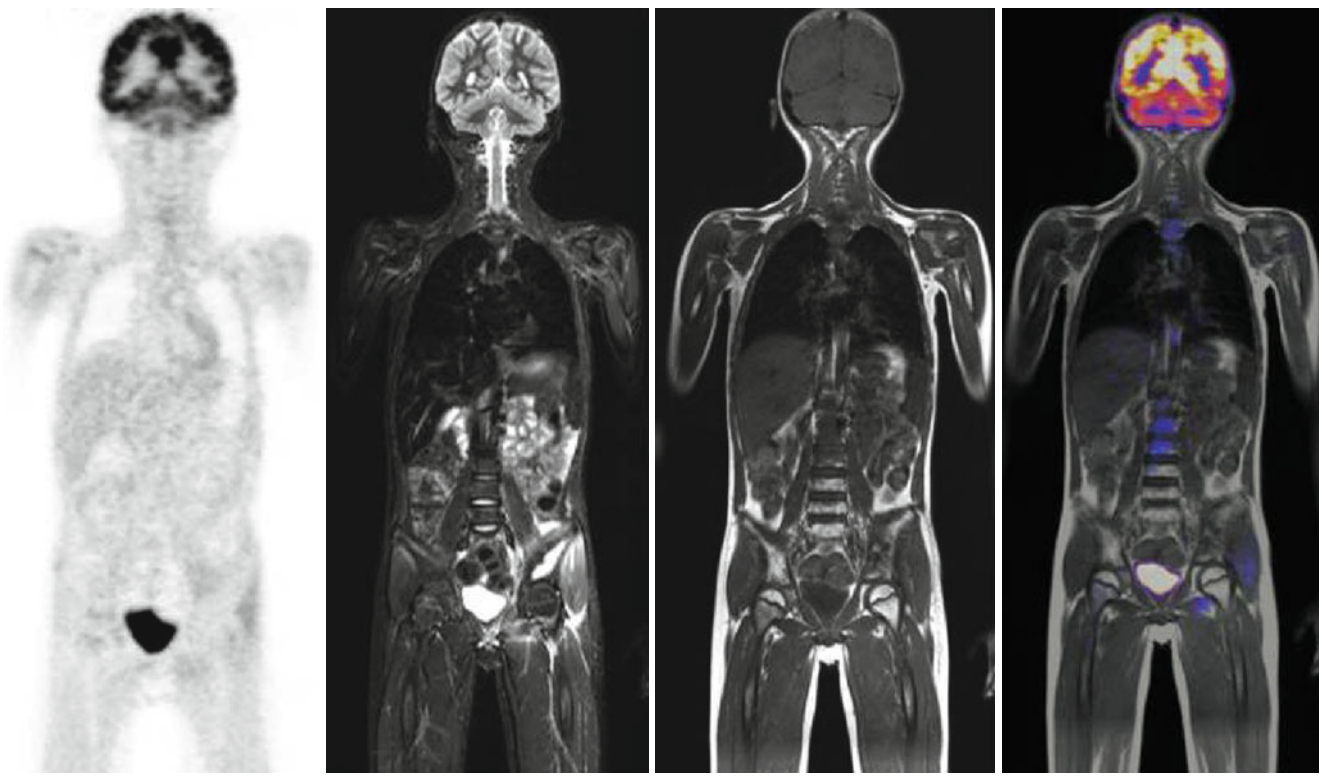

Fig. 9.23 After RCTx – 8 months later – tumor shrinkage is demonstrated in the MR component of the scan. However, a residual T1 hypointense/T2 hyperintense lesion is detected exhibiting no increased glucose utilization, indicating no active tumor. Further, a T2 hyperintense signal alteration is observed in the soft tissue surrounding the lesion indicating most probably an unspecific postactinic reaction

Recurrent Ewing's Sarcoma

Clinical History

Eight years old boy after RTx (12/2011) of a Ewing's Sarcoma of the cervical spine exhibiting intraspinal involvement. First scan (09/2012) was performed for restaging to exclude local or systemic recurrence. Consecutively patient received surgical treatment to resect the finding of the scan. Second scan (01/2013) was performed in the frame of follow up.

Imaging Technique

PET/MR 171 min and 153 min p.i. of 100 and 107 MBq 18F-FDG, 23 kg, 7 bed positions 3 min per bed position T1 VIBE Dixon for attenuation correction.

MR component first scan: cor T1 TSE, cor T2 STIR, sag T1 TSE post GD, cor T1 SPIR post GD; second scan: cor T1 TSE, cor T2 STIR.

Fig. 9.24 Coronal PET shows the lesion exhibiting a moderate focal 18F-FDG uptake (*arrow*) giving evidence of disease recurrence

Findings

There is focally increased glucose uptake in the cervical spine, corresponding to an intraspinal space occupying lesion also visible on the MR component of the scan (Fig. 9.24). The lesion is contrast agent enhancing (Fig. 9.25). The PET/MR fused image demonstrates the lesion exhibiting a moderate 18F-FDG uptake, suspect of recurrence of Ewing Sarcoma (Fig. 9.24). Surgical resection confirmed recurrent disease. The second scan performed after surgery showed no evidence of recurrent disease. The increased uptake shown on the fused images cervicaly and periclavicularly (Fig. 9.26) corresponds to fat tissue in the MR and corresponds unspecific uptake in brown fat.

Teaching Points

MRI is the method of choice to assess intraspinal involvement in disease. Simultaneous PET/MR imaging increased localization certainty of the hypermetabolic lesion shown in PET. Additionally it increased confidence in characterizing the space occupying lesion demonstrated in the MR component of the scan. The good distinction of fat tissue in the MR from other tissue (e.g. lymph nodes) helps in the evaluation of patients exhibiting increased glucose utilization in brown fat.

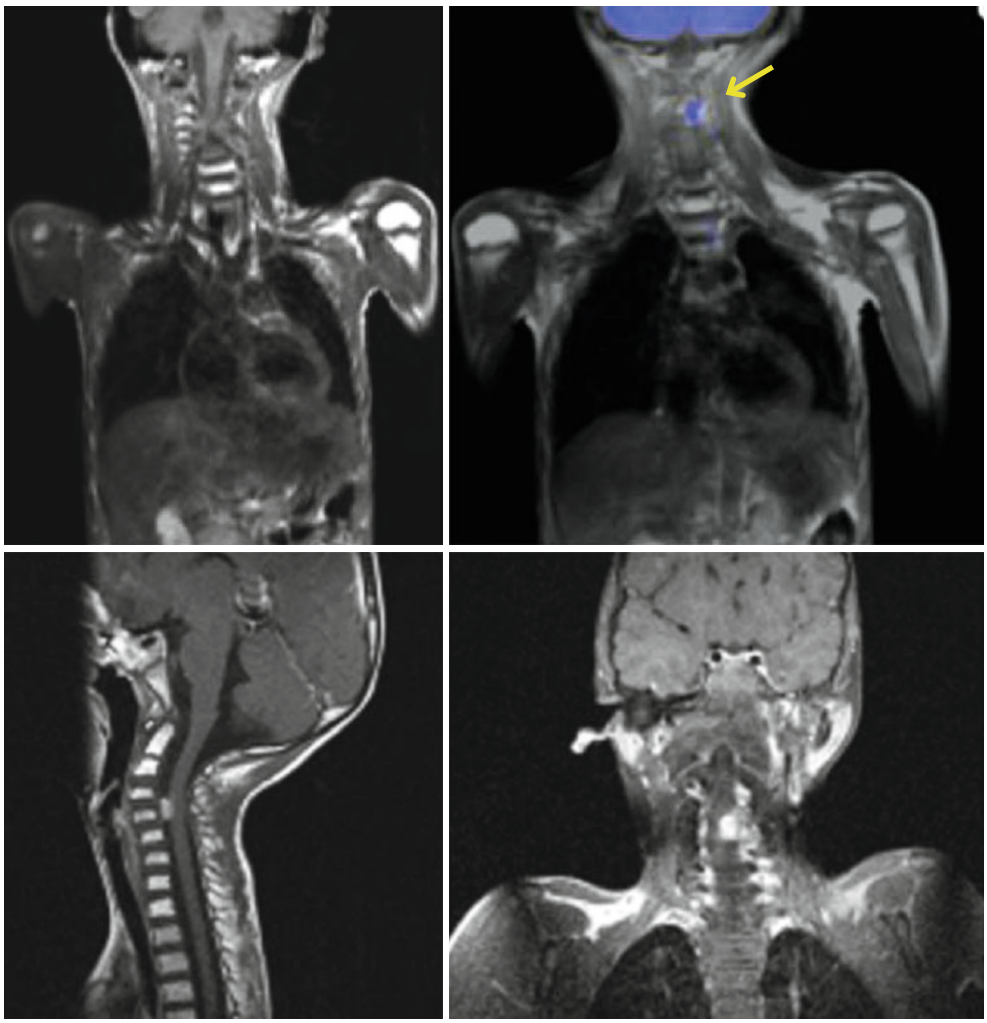

Fig. 9.25 Intraspinal lesion enhancing contrast shown most clearly in the sag T1 TSE post GD and in the cor T1 SPIR post GD (*both images in bottom row*). Coronal fused PET/MR images (*top right*) demonstrate the lesion exhibiting a moderate focal 18F-FDG uptake (*arrow*) giving evidence of disease recurrence

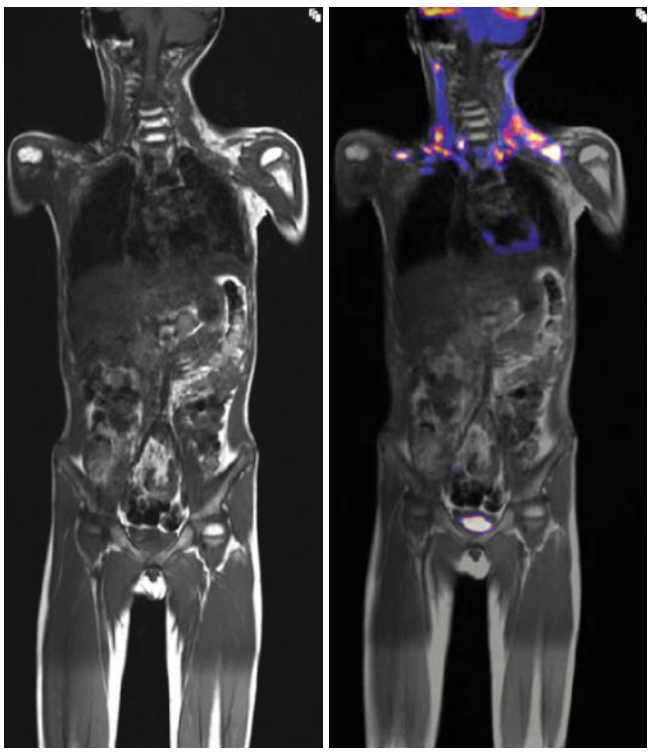

Fig. 9.26 Follow up PET/MR. The former lesion is not visible any more in condition after surgical excision. No new suspicious lesion was observed. Note the accurate correspondence of the increased glucose utilization cervical and periclavicular to fat tissue as shown in the MR component of the scan, indicating unspecific activity in brown fat

Multifocal Ewing Sarcoma

Clinical History

Fifteen years old patient treated with radiotherapy and chemotherapy for Ewing Sarcoma in the right humerus (until 09/2011). He was referred for restaging in the frame of follow up (03/2012).

Imaging Technique

PET/MR 136 min p.i. of 283 MBq 18F-FDG, 41 kg, 7 bed positions 3 min per bed position, T1 VIBE Dixon for attenuation correction.

MR component: cor T1 TSE, cor T2 STIR, sag T1 TSE, sag T2 STIR.

Findings

PET/MR raises suspicion of a multifocal recurrence of Ewing Sarcoma with hypermetabolic foci in multiple sites (Fig. 9.27). In all cases a typical T1 hypointense/T2 hyperintense signal alterations can be observed (Fig. 9.28).

Teaching Points

PET/MR is a valuable whole body imaging method for diseases which can involve multiple sites. The high sensitivity of MR in assessing bone marrow involvement adds in the high sensitivity of PET in restaging of Ewing Sarcoma. Furthermore the radiation exposure of PET/MR for pediatric patients is lower compared to PET/CT.

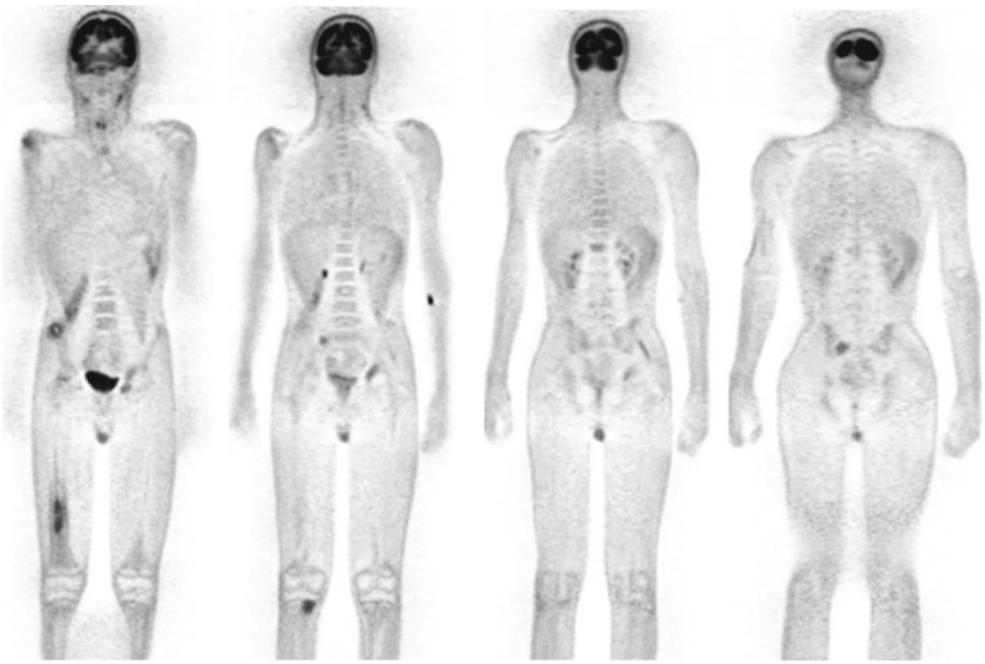

Fig. 9.27 Coronal PET/MR images at different levels showing hypermetabolic foci in the right femur, in both iliac bones, in the right medial tibia condyles, in the 12th thoracic vertebral bone and in the right sacral bone

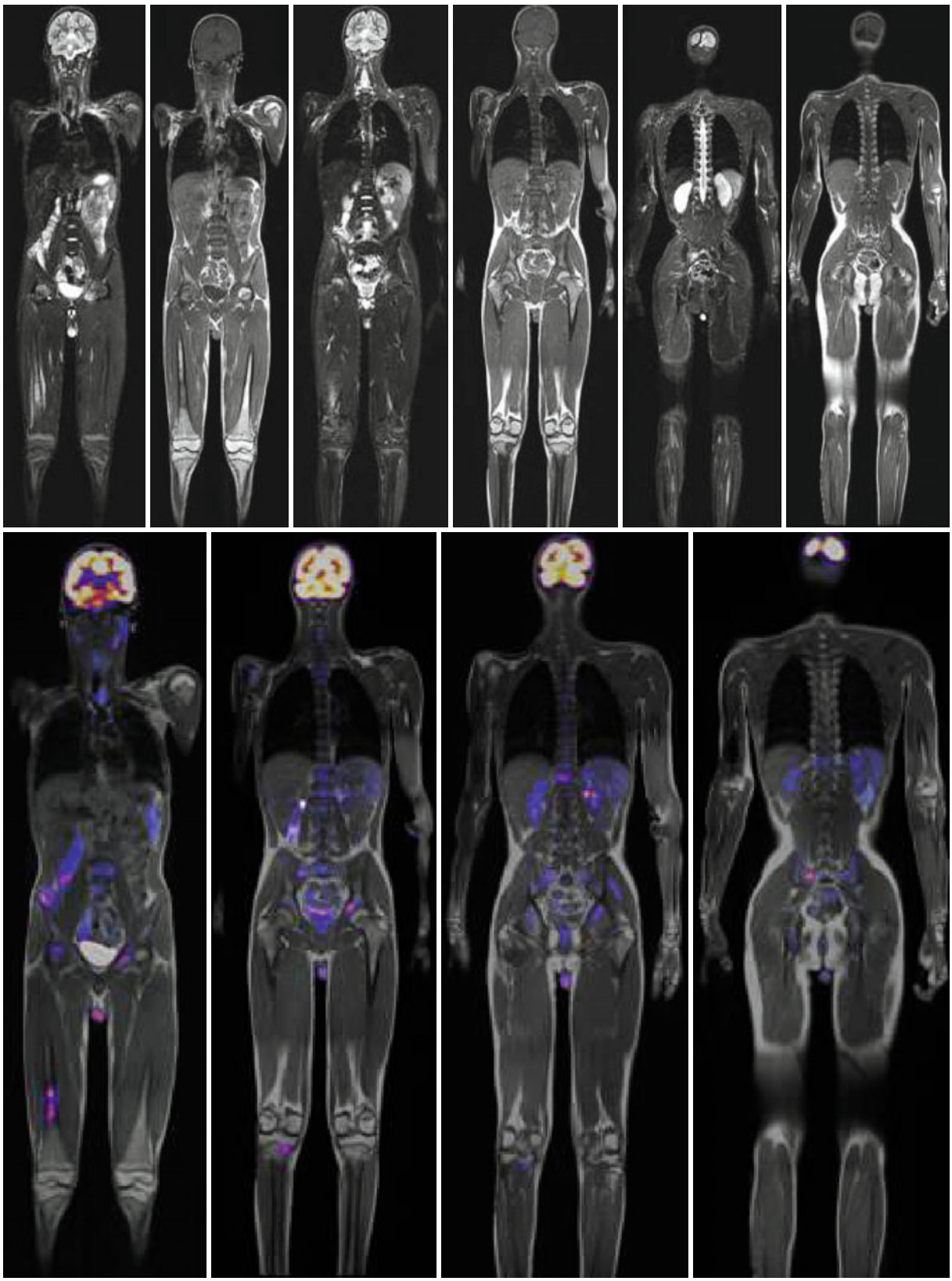

Fig. 9.28 cor T1 TSE, cor T2 STIR (*top*) and PET/MR fused images (*bottom*) of the sites suspected to be involved in the disease. All the hypermetabolic foci present with a T1 hypointense/T2 hyperintense signal alteration in MR suggesting bone marrow manifestations of Ewing Sarcoma. Additionally MRI provides detailed anatomical and diagnostic information. Note the T2 hyperintense signal alteration in the periost surrounding the manifestation in the right femoral bone suggesting periostal reaction

Treatment Follow-up of Lymphoma

Clinical History

Sixteen years old patient with Hodgkin lymphoma diagnosed after biopsy of a cervical lymph node referred for staging and follow up after two cycles of chemotherapy.

Imaging Technique

PET/MR 162 and 127 min p.i. of 327 and 387 MBq 18F-FDG, 60 kg, 5 bed positions 4 min per bed position T1 VIBE Dixon for attenuation correction.

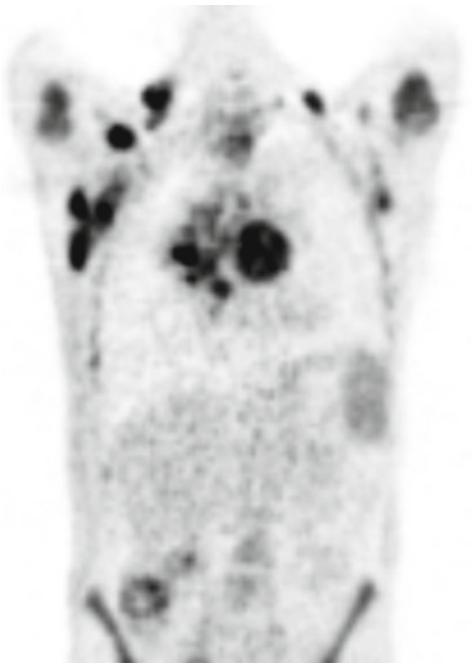

Fig. 9.29 Coronal PET demonstrates extensive FDG-uptake in cervical, axiallary and mediastinal lymph nodes

MR sequences in both scans: cor T2 STIR, ax VIBE fs post GD, thorax cor T2 haste fs.

Findings

In the pretherapeutic scan there are multiple foci of increased glucose utilization/enlarged lymph nodes in the cervical, axillary and mediastinal lymph node stations with infiltration of the sternum (Figs. 9.29, 9.31). Additionally in the MR component pleural effusion is observed. Further, increased homogenous uptake in the bone marrow can be noted indicating probably bone marrow activation, however bone marrow involvement can not be excluded.

In the scan after two cycles of CTx enlarged lymph nodes are demonstrated in the axilla in the MR component, however there is a decrease in number and size observed (Figs. 9.30 and 9.32). The lymph nodes exhibit tracer accumulation in the same range as that of blood pool (Fig. 9.30). The scan indicates a good response to chemotherapy.

Teaching Points

MRI has an equal performance to CT in imaging lymph node involvement in lymphoma. PET is a valuable staging and restaging method for FDG avid lymphomas. As the overall life expectancy of children with lymphoma can be long and in many cases not reduced compared to that of healthy population, it is important to keep radiation exposure as low as possible. Therefore, combining the anatomical MRI-information and the high accuracy of PET in detecting viable lymphoma tissue, could become the preferred choice compared to PET/CT when evaluating lymphoma in children.

Fig. 9.30 Coronal PET slices in different levels of the PET/MR after two cycles of CTx

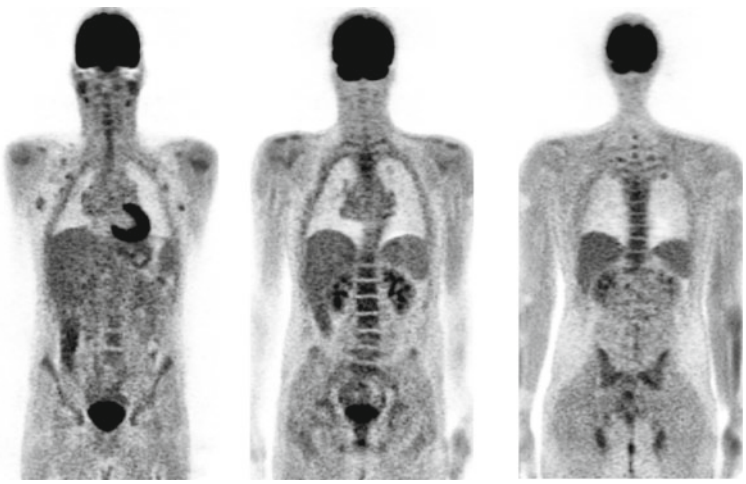

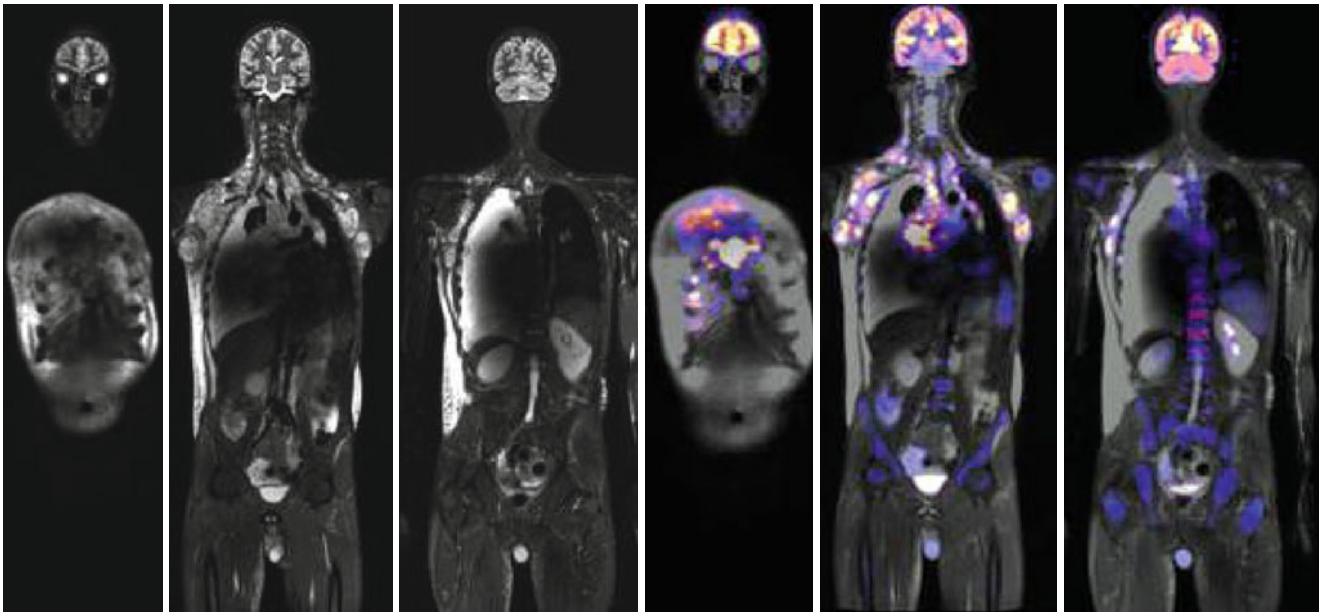

Fig. 9.31 Slices in different levels of the cor T2 STIR and PET/MR fused images. The enlarged lymph nodes are presenting as T2 hyperintense signal alterations in the MR component. Note the pleural effusion imaged in the MR component and the lymphoma manifestation destructing the sternum best seen in the fused images

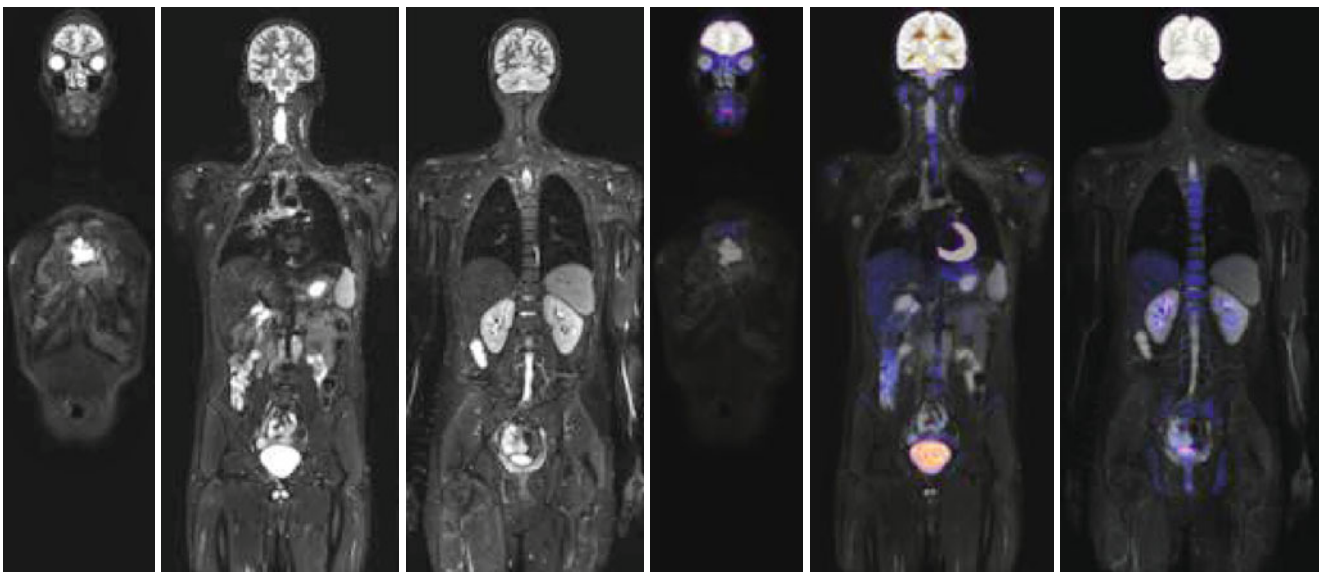

Fig. 9.32 PET/MR after two cycles of chemotherapy. Enlarged, T2 hyperintense lymph nodes in the axilla can be observed, however compared to the pretherapeutic scan they are reduced in number and size. The pleural effusion is resolved. Overall a good response to treatment can be reported

References

1. Pichler BJ, Kolb A, Nägele T, Schlemmer H-P (2010) PET/MRI: paving the way for the next generation of clinical multimodality imaging applications. J Nucl Med 51(3):333–336
2. Hirsch FW, Sattler B, Sorge I, Kurch L, Viehweger A, Ritter L et al (2013) PET/MR in children. Initial clinical experience in paediatric oncology using an integrated PET/MR scanner. Pediatr Radiol (in press)
3. Chawla SC, Federman N, Zhang D, Nagata K, Nuthakki S, McNitt-Gray M et al (2010) Estimated cumulative radiation dose from PET/CT in children with malignancies: a 5-year retrospective review. Pediatr Radiol 40(5):681–686
4. Kwee TC, Takahara T, Vermoolen MA, Bierings MB, Mali WP, Nievelstein RAJ (2010) Whole-body diffusion-weighted imaging for staging malignant lymphoma in children. Pediatr Radiol 40(10):1592–1602; quiz 1720–1721
5. Sinha S, Peach AHS (2010) Diagnosis and management of soft tissue sarcoma. BMJ 341(1):c7170–c7170
6. Tateishi U, Hosono A, Makimoto A, Nakamoto Y, Kaneta T, Fukuda H et al (2009) Comparative study of FDG PET/CT and conventional imaging in the staging of rhabdomyosarcoma. Ann Nucl Med 23(2):155–161
7. Baum SH, Frühwald M, Rahbar K, Wessling J, Schober O, Weckesser M (2011) Contribution of PET/CT to prediction of outcome in children and young adults with rhabdomyosarcoma. J Nucl Med 52(10):1535–1540
8. Denecke T, Hundsdörfer P, Misch D, Steffen IG, Schönberger S, Furth C et al (2010) Assessment of histological response of paediatric bone sarcomas using FDG PET in comparison to morphological volume measurement and standardized MRI parameters. Eur J Nucl Med Mol Imaging 37(10):1842–1853